FTIR Difference Spectra of *Wolinella succinogenes* Quinol:Fumarate Reductase Support a Key Role of Glu C180 within the "E-Pathway Hypothesis" of Coupled Transmembrane Electron and Proton Transfer†

Alexander H. Haas,‡ Ursula S. Sauer,‡,§ Roland Gross,∥,⊥ Jörg Simon,∥,# Werner Mäntele,△ and C. Roy D. Lancaster*,‡

Department of Molecular Membrane Biology, Max Planck Institute of Biophysics, Max-von-Laue-Strasse 3, D-60438 Frankfurt am Main, P.O. Box 55 03 53, D-60402 Frankfurt am Main, Germany, Institute of Microbiology, Johann Wolfgang Goethe University, Marie-Curie-Strasse 9, D-60439 Frankfurt am Main, Germany, and Institute of Biophysics, Johann Wolfgang Goethe University, Max-von-Laue-Strasse 1, D-60438 Frankfurt am Main, Germany

Received May 28, 2005; Revised Manuscript Received August 18, 2005

ABSTRACT: Electrochemically induced static FTIR difference spectroscopy has been employed to investigate redox-driven protonation changes of individual amino acid residues in the quinol:fumarate reductase (QFR) from *Wolinella succinogenes*. The difference spectra presented were taken in the mid-infrared region from 1800 to 1000 cm^{-1}, and the signals obtained represent transitions between the reduced and oxidized states of the enzyme. Analysis of the difference spectra shows evidence for structural reorganizations of the polypeptide backbone upon the induced redox reaction. Furthermore, spectral contributions were found above 1710 cm^{-1} where stretching vibrations of protonated carboxyl groups from aspartic or glutamic acid side chains absorb. With the help of site-directed mutagenesis and hydrogen/deuterium isotope exchange, it was possible to identify amino acid residue Glu C180, which is located in the membrane-spanning, diheme-containing subunit C of QFR, as being partially responsible for the derivative-shaped spectral feature with a peak/trough at 1741/1733 cm^{-1} in the reduced-minus-oxidized difference spectrum. This signal pattern is interpreted as a superposition of a protonation/deprotonation and a change of the hydrogen-bonding environment of Glu C180. This residue is the principal constituent of the recently proposed "E-pathway hypothesis" of coupled transmembrane proton and electron transfer in QFR [Lancaster, C. R. D. (2002) *Biochim. Biophys. Acta 1565*, 215−231]. Thus, the study presented yields experimental evidence which supports a key role of Glu C180 within the framework of the E-pathway hypothesis.

The enzyme quinol:fumarate reductase (QFR) participates in anaerobic respiration with fumarate acting as the terminal electron acceptor, and it is part of an electron transport chain which catalyzes the oxidation of various electron donor substrates such as NADH,[1] H_2, or formate (*1*, *2*). These electron transfer reactions are associated with the generation of a transmembrane electrochemical proton potential that can be used by the ATP synthase for energy storage in a manner analogous to that of aerobic respiration (*3*). QFR is a membrane protein complex that couples the two-electron reduction of fumarate to succinate (reaction 1) to the two-electron oxidation of quinol to quinone (reaction 2):

$$\text{fumarate} + 2H^+ + 2e^- \rightarrow \text{succinate} \quad (1)$$

$$\text{quinol} \rightarrow \text{quinone} + 2H^+ + 2e^- \quad (2)$$

QFR is also able to catalyze the reverse reaction in vitro (*4*) and thus also acts as a succinate:quinone reductase (SQR). SQR, also known as respiratory complex II, is involved in aerobic metabolism as part of the aerobic respiratory chain (*5*) and the citric acid cycle. Both enzymes, QFR and SQR, belong to the superfamily of succinate:quinone oxidoreductases [SQORs, EC 1.3.5.1 (*5*−*9*)].

QFR from *Wolinella succinogenes* comprises two hydrophilic subunits (A and B) and one hydrophobic, membrane-

† This work was supported by the Deutsche Forschungsgemeinschaft (SFB 472 "Molecular Bioenergetics") and the Max Planck Society.

* To whom correspondence should be addressed: E-mail: Roy.Lancaster@mpibp-frankfurt.mpg.de. Tel: +49-69-6303-1013. Fax: +49-69-6303-1002.

‡ Department of Molecular Membrane Biology, Max Planck Institute of Biophysics.

§ Present address: Abteilung Klinische Chemie und Klinische Biochemie in der Chirurgischen Klinik, Klinik der Universität, Nussbaumstrasse 20, D-80336 München, Germany.

∥ Institute of Microbiology, Johann Wolfgang Goethe University.

⊥ Present address: Biotest AG, Landsteinerstrasse 5, D-63303 Dreieich, Germany.

Present address: School of Biological Sciences, University of East Anglia, Norwich NR4 7TJ, U.K.

△ Institute of Biophysics, Johann Wolfgang Goethe University.

[1] Abbreviations: ATP, adenosine triphosphate; cmc, critical micelle concentration; FAD, flavin adenine dinucleotide; FTIR, Fourier transform infrared; Fum, fumarate; $^1H/^2H$, hydrogen/deuterium; IR, infrared; KP_i buffer, potassium phosphate buffer; NADH, (reduced) nicotinamide adenine dinucleotide; OD, optical density; QFR, quinol:fumarate reductase; RC, reaction center; SHE′, standard hydrogen electrode at pH 7; SQR, succinate:quinone reductase; SQOR, succinate:quinone oxidoreductase; vis, visible; WT, wild type.

10.1021/bi051011d CCC: $30.25
Published on Web 09/29/2005

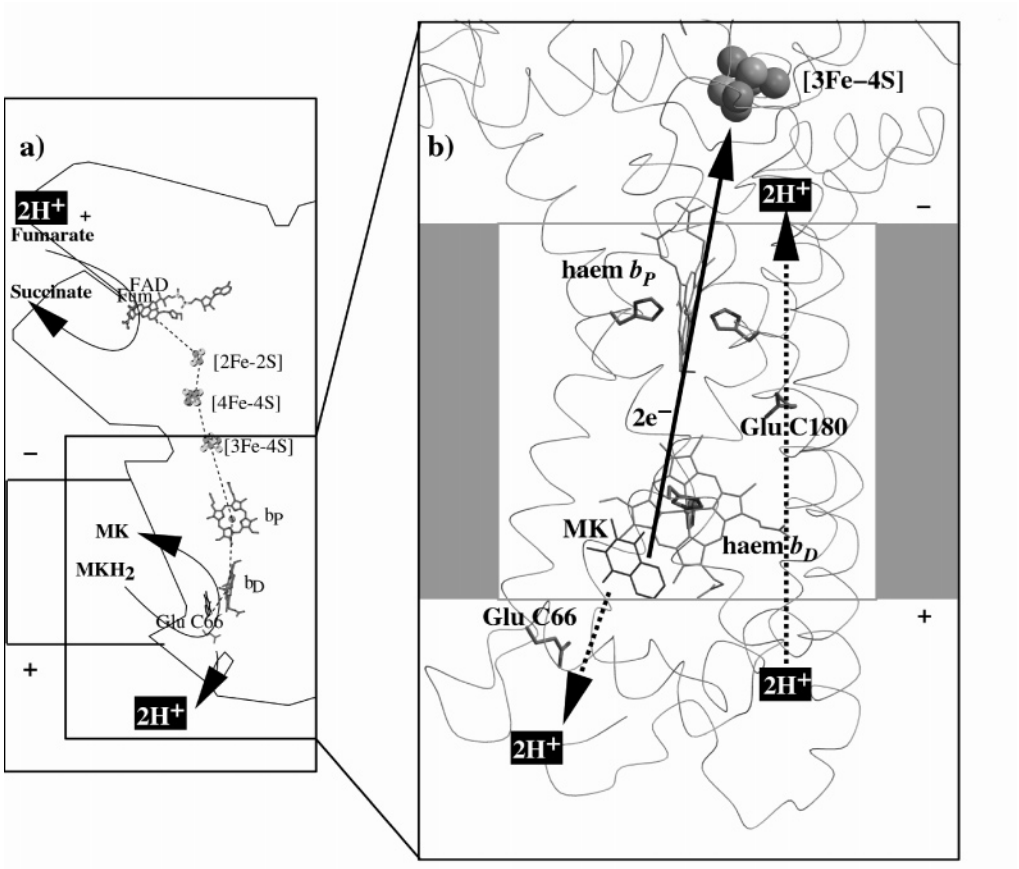

FIGURE 1: E-pathway hypothesis of coupled transmembrane proton and electron transfer in the QFR from *W. succinogenes*. The negative side of the indicated membrane is the bacterial cytoplasm; the positive side corresponds to the periplasm. (a) Hypothetical establishment of a transmembrane electrochemical potential (without an E-pathway) as suggested by the essential role of Glu C66 for menaquinol oxidation by *W. succinogenes* QFR (*11*). Panel a features the prosthetic groups of the *W. succinogenes* QFR dimer [coordinates as in 1QLA (*10*)]. Also indicated are the side chain of Glu C66 and a model of menaquinol (MKH_2) binding. The position of bound fumarate (Fum) is taken from PDB entry 1QLB (*10*). (b) Hypothetical cotransfer of one proton per one electron across the membrane (E-pathway hypothesis) (*15*). The two protons that are liberated upon menaquinol oxidation (MKH_2) are released toward the periplasmic side of the membrane via residue Glu C66. In compensation, coupled to electron transfer via the two heme groups, protons are transferred from the periplasm via the ring C propionate of the distal heme b_D and residue Glu C180 to the cytoplasm, where they counterbalance the two protons which are bound during fumarate reduction. In the oxidized state of the enzyme the E-pathway is required to be inactive.

integrated subunit C. The larger hydrophilic subunit A incorporates a covalently bound flavin adenine dinucleotide (FAD), the smaller hydrophilic subunit B contains three iron−sulfur clusters ([2Fe-2S], [4Fe-4S], and [3Fe-4S]), and the hydrophobic subunit C harbors two heme *b* groups. On the basis of their relative distance to the hydrophilic subunits, these heme groups are referred to as the "proximal" heme b_P and the "distal" heme b_D, respectively. The structure of QFR from *W. succinogenes* has been determined at 2.2 Å resolution by X-ray crystallography (*10*). The site of menaquinol oxidation of QFR is located close to the periplasmic side of the membrane in the vicinity of amino acid residue Glu C66 (where "C" indicates the C subunit) (*11*). The functional role and location of Glu C66 indicate that the two protons, which are liberated during menaquinol oxidation, are released to the periplasm and would thus lead to the generation of transmembrane proton potential, as two protons are invariably bound from the cytoplasm upon fumarate reduction. However, as discussed previously (*11*), experiments performed with inverted vesicles and proteoliposomes containing QFR indicated that quinol oxidation by fumarate is an electroneutral process (*12*−*14*). In an attempt to resolve this apparent contradiction, the so-called "E-pathway hypothesis" has been proposed (*15*) (see Figure 1). According to this hypothesis, the transfer of two electrons via the two QFR heme groups is strictly coupled to a compensatory, parallel transfer of two protons across the membrane via a proton transfer pathway, which is transiently open during the reduction of the two hemes and closed in the oxidized state of the enzyme. The two most prominent constituents of the proposed pathway were suggested to be the ring C propionate of the distal heme b_D and amino acid residue Glu C180.

In the context of the proposed E-pathway hypothesis, electrochemically induced FTIR difference spectroscopy was employed in this study to investigate the QFR from *W. succinogenes* with respect to coupled electron and proton transfer. The wild-type (WT) and particularly enzyme variant Glu C180 → Gln (abbreviated E180Q) were analyzed. Two additional variants [Glu C66 → Gln (E66Q) and Glu A270 → Gln (E270Q)], involving the replacement of Glu residues lining the menaquinol oxidation site and the fumarate reduction site, respectively, were included in the study for comparison.

Proton transfer within a protein usually occurs via networks of hydrogen bonds, which are established by ionizable amino acid side chains (e.g., Asp or Glu), heme propionates, and internal water molecules. Especially with

respect to protonated Asp or Glu side chains, the combined technique of electrochemistry and FTIR difference spectroscopy (*16*) is ideally suited to investigate their possible involvement in the enzymatic redox reaction (for recent reviews see refs *17* and *18*). The technique is sensitive enough to monitor the redox reaction on the level of single IR-active chemical bonds. In addition, no groups other than protonated aspartic (Asp) or glutamic (Glu) acid side chains (*19*) and a FAD carbonyl $\nu(C_4{=}O)$ vibration in the oxidized state (*20*, *21*) are expected to absorb in the relevant frequency range above 1710 cm^{-1}. The changes in absorbance, which occur during the redox reaction, are very small compared to the total IR bulk absorption. Thus, it is essential to compute difference spectra, which exclusively contain contributions of the affected vibrations. The majority of protein FTIR difference bands arises from the electrochemically induced redox changes in the vicinity of the redox-active sites (i.e., cofactors, prosthetic groups, or substrates).

The largest difference signals observed in the presented study are of the order of 0.3−0.5% of the total IR absorption (approximately 1 OD at 1648 cm^{-1}) while the smallest difference signals that can be resolved [i.e., the tentative ν(COOH) stretching vibrations] are of the order of approximately 0.01% or even less. This high sensitivity can be achieved since the different protein states are electrochemically adjusted in the infrared cuvette using the same sample.

In general, IR absorption spectra as well as IR difference spectra of such large systems as entire proteins are usually very diverse and complicated. To achieve a reliable band assignment for at least some of the observed bands, there are two powerful techniques which are also commonly used in a combined approach. One technique is isotopic labeling of the sample with, for example, ^{13}C, ^{15}N, or ^{18}O atoms or to perform a hydrogen/deuterium ($^1H/^2H$) isotope exchange via ^2H_2O buffers. The main object of these techniques is to change the physical mass of the labeled entity while maintaining the chemical properties. This altered mass is then reflected in shifted vibrational frequencies that can be observed in the IR spectra. The other technique is site-directed mutagenesis, which is used to modify the functional group of an amino acid residue and, thus, also modify its spectroscopic properties. In addition, the employed electrochemical cell allows monitoring individual redox-active groups by setting the appropriate electric potentials.

The combined method of FTIR spectroscopy and electrochemistry employed here as well as the mentioned strategies for IR band assignment are well established approaches and have previously been applied to several other membrane-bound enzymes, e.g., bacterial reaction centers (*22*), cytochrome *c* oxidase (*23*−*25*), ba_3 oxidase (*26*), NADH: ubiquinone oxidoreductase (*20*), cytochrome bo_3 (*27*, *28*), and the cytochrome bc_1 complex (*29*, *30*).

The results presented here concentrate on the role of amino acid residue Glu C180 in the mechanism of redox-driven coupled transmembrane electron and proton transfer of *W. succinogenes* QFR as it has been proposed in the context of the E-pathway hypothesis.

MATERIALS AND METHODS

Sample Preparation. Site-directed mutagenesis, cell growth of *W. succinogenes* wild-type and mutants, and purification of the respective enzymes have been described for WT QFR (*10*), for variant E180Q (C. R. D. Lancaster, U. S. Sauer, R. Gross, A. H. Haas, J. Graf, H. Schwalbe, W. Mäntele, J. Simon, and G. Madej, manuscript submitted for publication), for variant E66Q (*11*), and for variant E270Q (C. R. D. Lancaster, R. Gross, and J. Simon, manuscript in preparation), respectively. For spectroelectrochemical FTIR spectroscopy between pH 5.5 and pH 8, QFR was washed and concentrated in 100 mM potassium phosphate (KP_i) (Carl Roth GmbH & Co., Karlsruhe, Germany) buffer containing 100 mM KCl (Merck, Darmstadt, Germany) as supporting electrolyte and 1 mM *n*-dodecyl β-D-maltoside (Glycon Biochemicals, Luckenwalde, Germany) [cmc = 0.17 mM (*31*)] as detergent. Above pH 7.5, a 100 mM sodium borate (Merck, Darmstadt, Germany) buffer, containing 100 mM KCl and 1 mM *n*-dodecyl β-D-maltoside, was chosen. Samples with protein concentrations of up to 1.5 mM were prepared for the spectroscopic experiments. For the necessary washing cycles, Centrisart I filtration tubes (Sartorius, Göttingen, Germany) with a cutoff mass of 100 kDa and a volume of 2 mL were used. The final sample volume was adjusted in Vivaspin 500 μL concentrators (Vivascience, Hannover, Germany), also with a 100 kDa cutoff. Samples in ^2H_2O were prepared in an analogous way. Standard solutions (100 mM) of K_2HPO_4 and KH_2PO_4 (both anhydrous), which also contained 100 mM KCl, were made with ^2H_2O of 99.9% purity (Deutero GmbH, Germany). By titrating the two standard buffer solutions against each other, an observed pH_{obs} of 7 was set that corresponds to a p^2H value of 7.4 ($p^2H = p^1H + 0.4$) (*32*). Finally, the detergent was added to the buffer. The samples were then repeatedly concentrated and washed with ^2H_2O buffer until the calculated water content of the protein solution was well below 0.1%. Following the same $^1H/^2H$ isotope exchange strategy as for the cytochrome *c* oxidase from *Paracoccus denitrificans* (*23*), the extent of $^1H/^2H$ exchange was estimated to be of the order of 80%, which is in line with previous studies on other membrane-bound redox enzymes.

Electrochemistry. The electrochemically induced FTIR difference spectroscopy was performed in an ultrathin-layer spectroelectrochemical cell that was designed for combined FTIR and UV/vis spectrometry. The optical path length of this cell is variable and was of the order of 10 μm. For a more detailed description of this device, see refs *33* and *34*.

The surface of the gold grid working electrode has to be modified chemically prior to the experiment in order to prevent irreversible protein adsorption. Thus, the electrode was treated with a mercaptopropionic acid solution (Fluka, Switzerland) (2 mM in ethanol) (see ref *35* for further explanations). To enable fast redox reactions inside the spectroelectrochemical cell, a mixture of 15 redox mediators [tetrachlorobenzoquinone, 2,6-dichlorophenolindophenol, ruthenium hexaminchloride, 1,2-naphthoquinone, trimethylhydroquinone, menadione, 2-hydroxy-1,4-naphthoquinone, anthraquinone-2-sulfonate, benzyl viologen, methyl viologen, neutral red (cf. ref *24* and references cited therein), 5-hydroxy-1,4-naphthoquinone, duroquinone, anthraquinone, and anthraquinone-2,6-disulfonate (*36*) (Fluka, Switzerland)] was added to the protein solution. With the aid of this mixture, a (midpoint) potential range from roughly −0.4 to 0.3 V (vs SHE′) was densely covered. The total concentration of each

mediator substance in the experiment was approximately 40 μM. At this concentration level, an enhanced equilibration speed is achieved. Yet it is low enough to avoid any disturbing spectral contributions on behalf of the mediator substances, which was confirmed in control measurements containing the mediators but no protein sample (data not shown). For the experiments, the spectroelectrochemical cell was filled with 8 μL of protein solution, and the respective optical path length was checked spectroscopically after inserting the IR cuvette into the sample compartment. The applied potentials were measured with an Ag/AgCl/3 M KCl reference electrode, but all values quoted are potentials versus the standard hydrogen electrode at pH 7 (SHE′). Finally, a thin platinum plate served as a counter electrode, which was in electrical contact with the sample (via the electrolyte in the buffer) but situated outside the IR beam.

Spectroscopy. All IR difference spectra in the range of 1800−1000 cm^{-1} were recorded using a modified Bruker IFS 25 FTIR spectrometer that has been described in previous reports (*16*, *33*, *34*). Additional visible spectra were recorded with the same setup, which also includes a visible spectrophotometer (*33*); further experimental details are given in ref *11*. The sample compartment of the spectrometer has continuously been ventilated with dehumidified air to suppress any disturbing influence of water vapor absorption.

To keep the signals of interest above the noise level, the protein samples used had to be highly concentrated (∼1.5 mM). This is mainly necessary for two reasons: IR transmission experiments require a short optical path length because of the intense water absorption (i.e., the $^1H-O-^1H$ bending mode) around 1648 cm^{-1} (extinction coefficient $\epsilon = 18$ L mol^{-1} cm^{-1}) (*34*). Due to limited detector sensitivity, the thickness of the water layer should not exceed 10 μm to keep the absorbance around 1648 cm^{-1} below 1 OD (in ^2H_2O the situation is less critical since the corresponding absorbance band is shifted to ∼1210 cm^{-1}). Furthermore, the extinction coefficients of ν(COOH) modes are considerably small ($\epsilon = 200-400$ L mol^{-1} cm^{-1}) (*19*), and the ratio of solvent to protein concentration is about 40000.

Difference spectra were obtained by applying an initial (equilibrium) potential for which all of the cofactors of QFR were either fully reduced (full reductive potential −0.37 V) or fully oxidized (full oxidative potential +0.21 V). Before the respective single-beam spectrum was recorded after performing a potential step, the protein had to be given some time to equilibrate. Due to the various mediators, the very thin layer of protein solution and the gold grid surface modification, equilibration times were rather short (of the order of 1−3 min). Short equilibration times are necessary for good baseline stability. None of the presented data was smoothed or subjected to any spectral deconvolution. The only employed method to enhance the signal-to-noise ratio was to average multiple single-beam spectra; each single-beam spectrum is the result of the coaddition of 128 interferograms with a spectral resolution of 4 wavenumbers. Furthermore, a triangular apodization function and a zero-filling factor of 2 were applied. A noise level of below 5×10^{-5} is estimated by inspection of the baseline above ∼1750 cm^{-1}, where no noticeable signals are expected and found. The noise level is considerably higher in the region of strong solvent absorption as can be seen by sequentially recording baselines (data not shown). All measurements were performed at 5 °C, and all graphs were prepared with the software Origin 7 (OriginLab Corp.).

RESULTS

Electrochemically Induced IR and Visible Difference Spectra. An important criterion for the quality of the induced redox reaction and the associated difference spectra is their reversibility. In our experiments, all induced redox processes appear to be fully reversible under the applied experimental conditions since all collected difference spectra (for WT and variant enzymes) are completely symmetrical over the entire spectral range (symmetrical in the sense that exchanging final and initial state in the experiment results in a sign change of the accompanying difference spectrum; see Figure 2). This statement also includes the redox behavior of the two heme groups of QFR, as shown in the inset of Figure 2a, which shows an oxidized-minus-reduced as well as the respective symmetrical reduced-minus-oxidized difference spectrum in the visible range. The peak/trough feature at 411/428 nm (which is associated with the Soret band) and the peak at 561 nm (which is associated with the α-band) directly reflect the redox dependency of the visible absorption spectra of the heme *b* groups. By recording difference spectra at intermediate redox potentials between the reduced and oxidized state and plotting the absorbance changes of the Soret band and α-band against the applied external electrode potential (*33*), the midpoint potentials of the two heme *b* groups of QFR from *W. succinogenes* were determined to be −152 and −9 mV for the low- and high-potential heme, respectively (*11*). Because of the reversibility, oxidative and reductive titrations of the hemes yield the same values for the two heme midpoint potentials, and no hysteresis was observed. Following identical procedures, the corresponding values for the enzyme variant E180Q were −144 mV and +39 mV for the low- and high-potential heme, respectively (C. R. D. Lancaster, U. S. Sauer, R. Gross, A. H. Haas, J. Graf, H. Schwalbe, W. Mäntele, J. Simon, and G. Madej, manuscript submitted for publication). Thus, even in variant E180Q the high-potential heme was still fully oxidized at the experimentally applied full oxidative (equilibrium) potential of +0.21 V. In addition, for variants E66Q (*11*) and E270Q (data not shown) the values were unchanged with respect to WT QFR.

In the IR spectral range, data of QFR were recorded up to 1800 cm^{-1}, but there were no observable signals above ∼1750 cm^{-1}, independent of the applied electrode potential and pH. The obtained oxidized-minus-reduced (and, vice versa, reduced-minus-oxidized) difference spectra revealed numerous contributions in the entire spectral range between 1750 and 1000 cm^{-1}. Figure 2 shows electrochemically induced FTIR difference spectra of WT QFR and the three variant enzymes (i.e., E66Q, E270Q, and E180Q) in aqueous KP_i buffer at pH 7.

All presented spectra were normalized to a level that represents the average maximal absorbance difference (ΔAbs) in the amide I range of all difference spectra that have been selected for presentation. Since the amplitude ratio of individual pairs of difference bands is not perfectly conserved in independent experiments (measuring the same type of enzyme, i.e., WT or a specific variant, at the same pH and

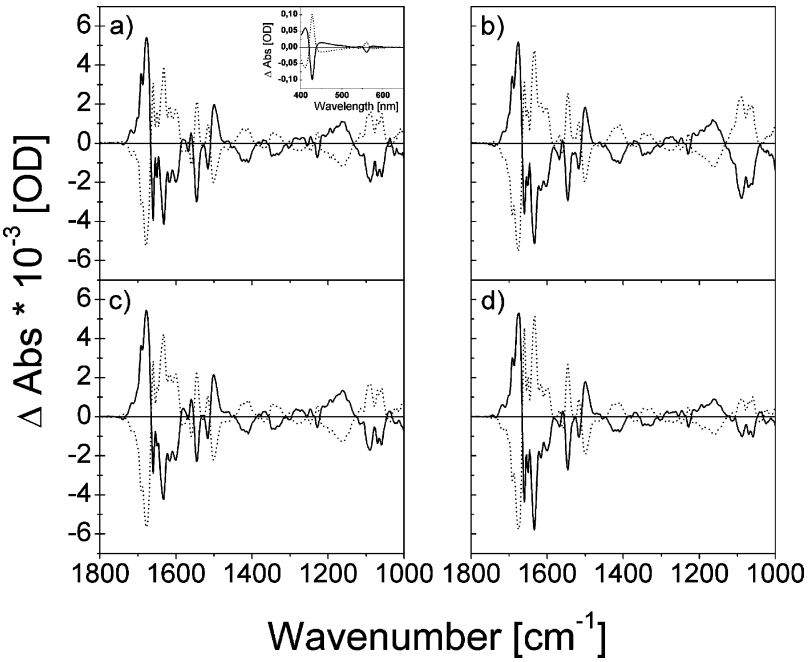

FIGURE 2: Electrochemically induced FTIR difference spectra (from 1800 to 1000 cm^{-1}). Reversible oxidized-minus-reduced (solid line) and reduced-minus-oxidized (dashed line) FTIR difference spectra of QFR WT at pH 7 (a), enzyme variant E66Q at pH 7 (b), enzyme variant E270Q at pH 7 (c), and enzyme variant E180Q at pH 7 (d). Reference electrode potentials for the shown FTIR difference spectra were +0.21 V (full oxidative potential) and −0.37 V (full reductive potential). Positive bands belong to the final state and negative ones to the initial state. In a reduced-minus-oxidized difference spectrum all positive bands belong to the reduced state while all negative bands belong to the oxidized state (and vice versa). The inset of panel a shows the corresponding visible difference spectra of QFR WT at pH 7 (from 400 to 650 nm). The heme difference band associated with the Soret band is located at 411/428 nm and the respective one for the α-band at 561 nm.

reference potentials), scaling of the difference spectra for comparison is not straightforward but always a compromise, as it cannot satisfactorily be achieved on the basis of a single difference band. This applies as well for the heme difference bands in the visible range, as the ratio of difference bands originating from the Soret band and α-band, respectively, is not constant in all experiments (data not shown). Thus, the scaling was performed on the basis of the large absorbance changes in the amide I region as has been done in other studies (e.g., refs *37*−*39*). The deviations between the different spectra are small compared to the overall absorbance differences and might be related to the individual protein concentration, sample layer thickness, and slightly different mediator concentration in the particular experiment.

The signal pattern in the region around 1648 cm^{-1} appears to be barely affected by the strong water absorbance (see Figure 2), although an elevated noise level around 1648 cm^{-1} can be seen in the baseline (data not shown). Yet the observed bands in the difference spectra in the amide I range are comparatively narrow and well reproducible. Thus, it is unlikely that the difference signals around 1648 cm^{-1} are not initiated by redox-dependent absorbance changes of the QFR sample. In ^2H_2O, the related region of increased noise (i.e., the region of the $^2H-O-^2H$ bending mode) can be found around 1210 cm^{-1} in the IR absorbance spectrum (data not shown).

Regarding the results presented here, we shall concentrate on the relevant contributions of acidic residues. In addition, a detailed tentative assignment of infrared bands in the presented QFR difference spectra is given in Table 1 and in more detailed, textual form as Supporting Information.

Amide I Contributions and Secondary Structure Elements. The most prominent spectral feature that can be observed for all investigated QFR samples (i.e., WT, E66Q, E270Q, and E180Q) in ^1H_2O and ^2H_2O buffer is a series of large well-pronounced positive and negative bands between approximately 1700 and 1475 cm^{-1} (see Figures 2 and 3). For a basic assignment of IR bands, we have to consider the relevant spectral regions in which contributions of the protein are expected: In the observed IR range between 1800 and 1000 cm^{-1} the amide I mode (primarily C═O stretching vibrations) of QFR contributes between approximately 1690 and 1615 cm^{-1} and peaks at 1656 cm^{-1} (IR absorbance spectrum not shown), which is indicative of predominantly α-helical secondary structure elements (*18*). The strong difference bands, especially at 1678 and 1632 cm^{-1}, in the amide I region can be assigned to vibrations of the polypeptide backbone, and thus those difference bands indicate local structural reorganizations of the protein, which are triggered by the induced redox reaction (*16*).

Effects of $^1H/^2H$ Isotope Exchange. Upon $^1H/^2H$ isotope exchange the difference spectra of WT QFR show pronounced deviations compared to the spectra in ^1H_2O buffer (see Figure 3). These spectral differences are also found in the respective difference spectra of the variant enzymes (data not shown).

KP_i Buffer. Below 1200 cm^{-1} the main spectral contributions are two broad bands with maximum intensity at 1162/1088 cm^{-1} (see Figure 2), which are caused by the potassium phosphate buffer. The difference signals originate from PO modes of the deprotonated phosphate buffer, which reflect proton uptake of the protein (this might also include redox-induced protonation changes of the FAD prosthetic group of QFR or enzyme-bound quinone molecules) as well as proton uptake of the mediator molecules in the course of the redox reaction (*23*, *26*, *29*).

Table 1: Summary of Tentative *W. succinogenes* QFR WT IR Band Assignments in ^1H_2O Buffer at pH 7[a]

wavenumber (cm^{-1})	redox state	tentative assignments
1738	red	Glu C180; ν(C═O)
1732	ox	Glu C180; ν(C═O)
1718	ox	FAD; $\nu(C_4{=}O)$
		Asp/Glu; ν(C═O)
1702	ox	heme prop; ν(C═O)
		Asn; ν(C═O)
1692	ox	Arg; $\nu_{as}(CN_3H_5^+)$
		heme prop; ν(C═O)
		Asn/Gln; ν(C═O)
1678	ox	amide I; turns and β-sheets
1660	red	Gln; ν(C═O)
1650	red	Arg; $\nu_s(CN_3H_5^+)$
1632	red	amide I; β-sheets
1617	red	heme vinyl; $\nu(C_\alpha{-}C_\beta)$
		Tyr−OH; ν(CC) δ(CH)
		Asn/Gln; $\delta(NH_2)$
1601	red	Gln; $\delta(NH_2)$
		Tyr−OH; ν(CC)
1582	ox	Asp/Glu; $\nu_{as}(COO^-)$
1576	ox	Asp/Glu; $\nu_{as}(COO^-)$
1560	ox	heme prop/Asp/Glu; $\nu_{as}(COO^-)$
1545	red	heme porph; $\nu(C_bC_b)$ and/
		or $\nu_{as}(C_aC_m)$
1516	red	FAD; $\delta(C_6{-}H)$ and $\delta(C_9{-}H)$
		Tyr−OH; ν(CC), δ(CH)
1501	ox	Tyr−O^-; ν(CC), δ(CH)
1462	ox	heme porph; $\nu_s(C_aC_m)$
1438	red	heme porph; $\nu(C_aC_b)$
1426	red	Pro; ν(CN)
		Trp; δ(NH), ν(CC), δ(CH)
1418	red	Pro; ν(CN)
1410	red	Gln; ν(CN)
1370	ox	heme prop/Asp/Glu; $\nu_s(COO^-)$
1348	red	Trp
1340	red	Trp
1330	red	Trp
1276	ox	Tyr−O^-; ν(C−O), ν(CC)
1267	ox	Tyr−O^-; ν(C−O), ν(CC)
1256	red	Tyr−OH; ν(C−O), ν(CC)
1162	ox	buffer; P═O
1088	red	buffer; P═O

[a] Multiple assignments are given for several vibrations which represent possible alternatives or additional contributions at the same wavenumber. Band affiliations to the corresponding redox state are indicated for the reduced (red) and oxidized (ox) state. The subscripts "as" and "s" indicate antisymmetric and symmetric vibrations, respectively. Porphyrin and propionate are abbreviated as "porph" and "prop", respectively. The labeling of heme *b* atoms is analogous to that in ref *43*. For tentative assignments of heme vibrations, see refs *42*, *43*, and *45*. See text and Supporting Information for references and for details of the other assignments.

Heme Propionates. Protonated heme propionates, which might be of functional importance with respect to redox-coupled proton transfer within the QFR enzyme, are expected to contribute between 1700 and 1665 cm^{-1} (*41*). This region overlaps with the amide I vibrations and is dominated by the large negative difference signal at 1678 cm^{-1} (see Figure 3), which makes it difficult to assign, even tentatively, contributions of any protonated heme propionates. The deprotonated forms of the propionates exhibit antisymmetric $\nu_{as}(COO^-)$ (between 1620 and 1540 cm^{-1}) and symmetric $\nu_s(COO^-)$ vibrations (between 1420 and 1300 cm^{-1}) (*41*). Tentative assignments of heme propionate bands are complicated since ionized Asp or Glu side chain contributions are expected at comparable frequencies (*19*). QFR enzyme exhibits various signals in the respective regions, and the small signals in the oxidized state at 1560 cm^{-1} and around 1370 cm^{-1} are conceivable $\nu_{as}(COO^-)$ and $\nu_s(COO^-)$ heme propionate signals. Presently, it is not possible to unequivocally resolve and assign contributions of ionized propionates to the observed difference bands.

Amino Acid Residues. The difference signals which are indicative of protonated Glu or Asp side chains appear above 1710 cm^{-1} in ^1H_2O buffer (see Figure 4), and they are shifted to lower wavenumbers in ^2H_2O buffer (see inset of Figure 3) as expected for this assignment (*19*). Hence, upon $^1H/^2H$ isotope exchange, the signals begin to overlap strongly with the large difference band in the amide I region (see inset of Figure 3). The respective vibrations of the ionized forms of Asp and Glu are expected between 1580 and 1560 cm^{-1} for the antisymmetric and between 1420 and 1400 cm^{-1} for the symmetric mode (*19*). In QFR, tentative Glu or Asp $\nu_{as}(COO^-)$ signals are found in the oxidized state at 1582, 1576, and 1560 cm^{-1} in ^1H_2O and at 1585 cm^{-1} in ^2H_2O. In the range of the symmetric $\nu_s(COO^-)$ mode in the reduced-minus-oxidized difference spectrum, only positive bands are found in both buffer types. In principle, the symmetric modes should exhibit the same sign as the corresponding antisymmetric vibrations if a particular acidic group undergoes a redox-induced protonation change. On the other hand, it cannot be ruled out that a specific vibration is canceled out by an additional contribution of opposite sign.

Influence of Amino Acid Exchanges on FTIR Difference Signals in the Range of ν(COOH) Modes. In the scope of this study, the most interesting spectral region is that of protonated Glu and Asp side chains, which is depicted in Figure 4. All four discussed enzyme types (WT, E66Q, E270Q, and E180Q) show contributions in their FTIR difference spectra in the range between 1760 and 1720 cm^{-1} (same data as in Figure 2). QFR WT exhibits a derivative-shaped pair of difference bands with similar width and amplitude at 1738/1732 cm^{-1} in ^1H_2O (see inset of Figure 4). In ^2H_2O at p^{2}H 7.4, the positive contribution in the reduced state is lost, and the signal is broadened and shifted to lower wavenumbers (approximately to 1734 cm^{-1}; see inset of Figure 3). Compared to WT QFR, the difference spectrum of the enzyme variants E66Q and E270Q exhibits a similar signal pattern with minor differences, which may be attributed to imperfect scaling and baseline variations (see Figure 4). In contrast, the replacement of residue Glu C180 by a glutamine leads to a completely different signal pattern. The shape of the difference band is reversed compared to the spectra of WT, E66Q, and E270Q, with peaks now at 1743/1735 cm^{-1}. Upon $^1H/^2H$ exchange, the band structure of E180Q is also slightly broadened and shifted to lower wavenumbers (1738 cm^{-1}; data not shown). For all enzyme types, the peak around 1718 cm^{-1} in ^1H_2O is shifted to lower wavenumbers by approximately 10 cm^{-1} upon $^1H/^2H$ exchange (see Figure 3 plus inset; data not shown for enzyme variants).

To specify the spectral effects of the introduced mutations E66Q, E270Q, and E180Q, double difference spectra of WT and the respective variant spectra were calculated. In theory, the bands that are visible in this type of double difference spectra can solely be attributed to the spectral differences induced by the single mutation. In practice, this would also imply perfect scaling of the corresponding difference spectra,

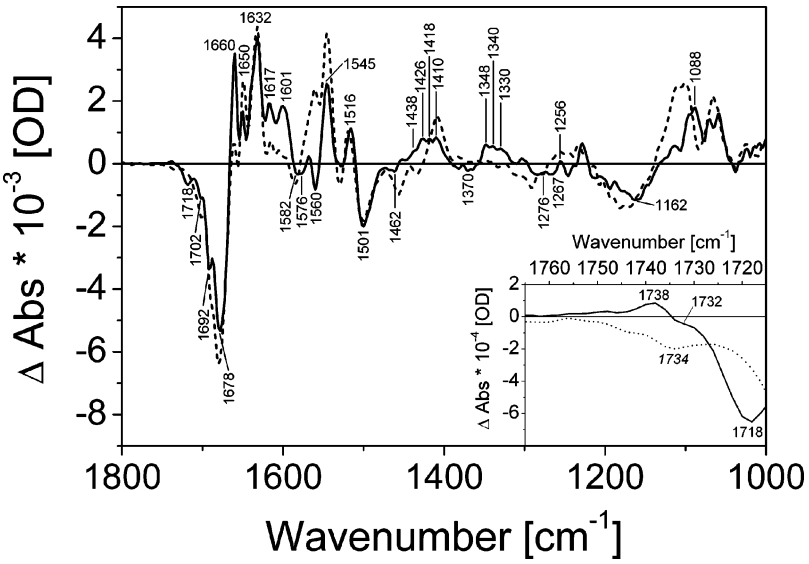

FIGURE 3: Electrochemically induced FTIR difference spectra of QFR WT in ^1H_2O and ^2H_2O (from 1800 to 1000 cm^{-1}). Reduced-minus-oxidized FTIR difference spectra of QFR WT at pH 7 (solid line) and at an observed pH_{obs} of 7 (which corresponds to p^2H 7.4; dashed line). The inset shows the same data in the wavenumber range from 1765 to 1715 cm^{-1}. Reference electrode potentials for the shown FTIR difference spectra were +0.21 V (full oxidative potential) and −0.37 V (full reductive potential). The wavenumbers of the bands in ^1H_2O as assigned in the text and Table 1 are indicated in the figure; bands in ^2H_2O are in italic type.

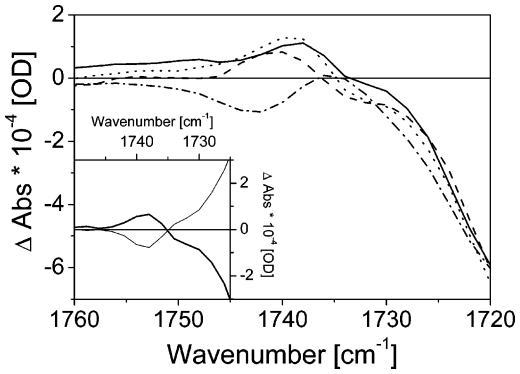

FIGURE 4: Electrochemically induced FTIR difference spectra (from 1765 to 1715 cm^{-1}). Overlay of reduced-minus-oxidized FTIR difference spectra of QFR WT (solid line), E66Q (dashed line), E270Q (dotted line), and E180Q (dashed−dotted line) at pH 7. Reference electrode potentials for the shown FTIR difference spectra were +0.21 V (full oxidative potential) and −0.37 V (full reductive potential). The inset features the same data as in the main figure but with a slight baseline correction. In addition, the data are supplemented with the corresponding oxidized-minus-reduced FTIR difference spectrum (thin line).

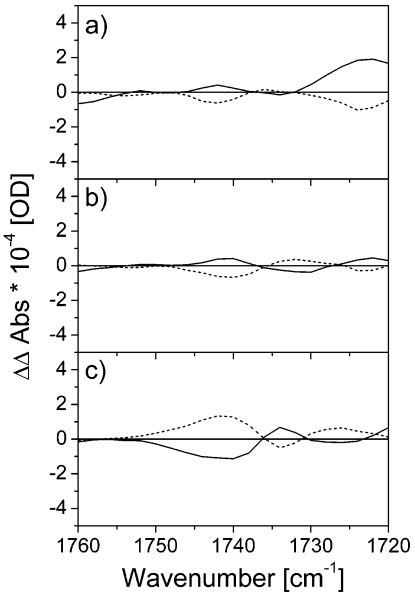

FIGURE 5: FTIR double difference spectra (from 1765 to 1715 cm^{-1}) of QFR. Oxidized-minus-reduced (solid line) and reduced-minus-oxidized (dashed line) FTIR double difference spectra of (a) WT minus E66Q, (b) WT minus E270Q, and (c) WT minus E180Q at pH 7. Reference electrode potentials for the shown FTIR double difference spectra were +0.21 V (full oxidative potential) and −0.37 V (full reductive potential). The data shown here are based on the data presented in Figure 2 but with corrected baselines (i.e., where necessary, a constant of the order of the noise level was subtracted to guarantee zero crossings of the pairs of double difference spectra at the same wavenumber; this procedure is identical with setting the spectra to zero at wavenumbers around 1760 cm^{-1} and above where no further signals were observed).

which is not a straightforward task in some cases. In Figure 5, double difference spectra for WT minus E66Q, E270Q, and E180Q are shown, which correspond to the back and forward direction of the redox reaction. The double difference spectrum of WT minus E66Q emphasizes the similarities of E66Q and WT spectra in the region above 1730 cm^{-1}. It is difficult to decide whether the deviation, which appears below 1730 cm^{-1}, is potentially significant, and is thus an effect of the mutated residue, or simply an artifact due to imperfect scaling of the two sets of spectra. In principle, the characteristics of the double difference spectra of WT minus E66Q and WT minus E270Q are very similar with respect to the frequency position of positive and negative residual difference signals. The small difference signals that can be seen around 1740 cm^{-1} in Figure 5a,b are due to slightly different positions of the peaks around 1740 cm^{-1} as can already be seen in Figure 4. Various reasons are conceivable for the slightly different peak positions: First, the limited spectral resolution of the FTIR spectrometer, which was 4 cm^{-1} (i.e., a data point separation of 2 cm^{-1}), has to be considered. Second, the signals of protonated carboxyl groups are pH sensitive (see also Figure 6). The QFR protein complex has many buffering groups itself, and different protein concentrations in the individual experiment might

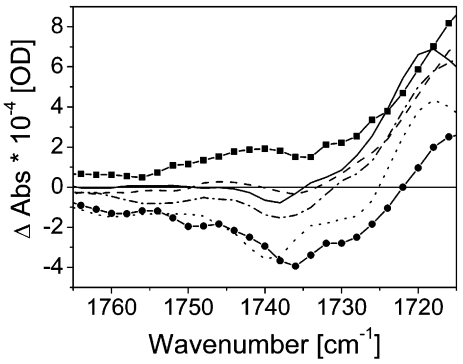

FIGURE 6: pH dependence of electrochemically induced FTIR difference spectra (from 1765 to 1715 cm^{-1}). Overlay of oxidized-minus-reduced FTIR difference spectra of QFR WT at pH 5.5 (squares), pH 6 (dashed line), pH 7 (solid line), pH 7.5 (dashed−dotted line), pH 8.5 (dotted line), and pH 8.8 (circles). Reference electrode potentials for the shown FTIR difference spectra were +0.21 V (full oxidative potential) and −0.37 V (full reductive potential).

thus lead to small variations of the sample pH. This effect would be more pronounced in the vicinity of the isoelectric point of the QFR protein complex, which is pH 6.0 (*47*). Furthermore, signals of COOH groups with lower frequencies are less isolated and instead more hydrogen-bonded, which also indicates higher solvent accessibility and thus a higher sensitivity for pH changes.

Inspection of the double difference spectrum of WT minus E270Q (see Figure 5b) underlines the result that the WT and variant spectrum are indeed very similar, making it unlikely that Glu A270 undergoes any environmental or protonation changes in the course of the induced reaction.

A double difference spectrum of WT and E180Q (see Figure 5c) unequivocally indicates the dramatic effect that the mutation E180Q has on the signal pattern of the electrochemically induced FTIR difference spectra of QFR in the spectral range of protonated carboxylic acid groups. Compared to the other two variants, the amplitude of the double difference signal of WT minus E180Q above 1730 cm^{-1} is sufficiently above the noise level to be considered significant, and the observed difference signal cannot be explained by the scaling difficulties mentioned above, baseline effects, or pH variations.

pH Dependency of FTIR Difference Signals in the Range of ν(COOH) Modes. Figure 6 shows the pH dependency of the QFR WT enzyme in the frequency range of protonated carboxyl groups between pH 5.5 and pH 8.8. With increasing pH, the positive peak around 1740 cm^{-1} diminishes and a broad negative band develops. At pH 6, the observed signals are minimal, and the biggest changes occur between pH 7.5 and pH 8.5. This pH-dependent behavior yields further support for the assignment of the respective difference bands found above 1725 cm^{-1} to protonated carboxylic acid groups of Glu and Asp side chains. It is also likely that multiple acidic residues are involved in the observed signal pattern, since different groups could contribute at different pH values. Also the spectral feature, which is centered around 1718 cm^{-1} at neutral pH, is affected by pH variation with respect to its position and intensity and becomes smaller with increasing pH. This could be due to underlying signals (of Asp or Glu side chains) or could reflect a pH dpendence of the tentatively assigned FAD signal.

DISCUSSION

Comparison of FTIR Difference Spectra of WT and Variant QFR and Redox-Induced Conformational Changes of the Enzyme. We have investigated WT and three different variant QFR enzymes from *W. succinogenes* by electrochemically induced FTIR difference spectroscopy. The IR data obtained of WT and variant enzymes correspond very well, and no major differences in the overall band pattern were observed (except for the presented differences that are related to the absence of protonated/deprotonated carboxylic acid groups in the three enzyme variants, discussed below). This result underlines the consistency and the reproducibility of the reduced-minus-oxidized (and vice versa) difference spectra. The same consistency was also found for all spectra measured in ^2H_2O.

For the enzyme variant E66Q, it was found by three-dimensional X-ray crystallography that it does not feature significant structural changes with respect to the WT structure (both oxidized) (*10*, *11*). Comparison of the FTIR difference spectra of the four presented enzyme types (see Figure 2) indicates that the conformational changes, which occur upon reduction, as judged by the difference signals in the amide I range, are the same for WT, E180Q, E66Q, and E270Q.

As mentioned above, all four enzyme types (WT and variants) have a relatively large redox-linked difference band in the amide I range in common, which features a zero crossing at approximately 1663 cm^{-1} (see Figure 2). This signal can be interpreted in terms of a conformational reorganization of the enzyme upon reduction. But the assignment is tentative as there is no crystal structure of the reduced form of QFR available so far. In a similar experiment on the heme−copper oxidases cytochrome aa_3 from *Rhodobacter sphaeroides* and the ubiquinol oxidase cytochrome bo_3 from *Escherichia coli*, which involved smaller absorbance changes (but with a comparable total IR absorbance) upon redox reaction in the amide I region, the number of peptide bonds involved in a redox-induced conformational change was estimated to be three to five (*48*). Even if a comparable number of peptide bonds were involved in the redox-dependent conformational changes of QFR, it is not evident how noticeably the induced conformational change would affect the structure of QFR. Generally speaking, just very few peptide bonds could serve as a hinge and thus enable a movement of an otherwise rigid domain of the protein, and only those peptide bonds involved in the hinge region would give rise to signals in the IR difference spectrum (*18*). A possible candidate for such a domain movement in QFR is the capping domain in the hydrophilic subunit A, which has been shown to be susceptible for larger conformational changes (*49*). In addition, when difference bands in the amide I region are assigned to conformational changes of the protein, it is possible that some (even large) conformational changes might contribute to the IR difference spectra in such a way that they cancel each other out, and hence the changes would not be adequately reflected in the IR difference spectrum (*18*). Thus, in the absence of additional information, such as the structure of the reduced QFR enzyme, the intensity of the involved difference bands is not sufficient to make a reliable statement about the extent of the underlying structural changes of QFR, which might be induced upon the redox reaction at the working electrode.

Effects of $^1H/^2H$ Isotope Exchange in QFR WT and Implications for Conformational Changes. The $^1H/^2H$ isotope exchange behavior of QFR can serve as another possible source of information on conformational changes of the enzyme. This exchange occurs passively via diffusion and rinsing of the sample with ^2H_2O-based buffer but can also be actively influenced via redox-induced conformational changes of the enzyme. Such exchange processes can be triggered electrochemically in the spectroelectrochemical cell and monitored with the help of FTIR spectroscopy.

All protein samples that have been prepared in ^2H_2O buffer still contain a substantial amount of ^1H_2O, although the samples have previously been thoroughly washed with ^2H_2O. This is reflected in the IR absorbance, which shows a residual ^1H_2O infrared band at 1648 cm^{-1} (i.e., the $^1H-O-^1H$ bending mode) of varying size depending on the individual preparation (data not shown). When the experiment is started by taking IR spectra at oxidative and reductive potentials, the corresponding difference spectra reveal an unstable baseline that exhibits three broad bands (i.e., the $^1H-O-^1H$ bending mode at 1648 cm^{-1}, a mixed $^1H-O-^2H$ mode at 1456 cm^{-1}, and the $^2H-O-^2H$ bending mode at 1210 cm^{-1}; data not shown) which directly show the decrease of ^1H_2O and the increase of ^2H_2O content in (and around) the area of the IR beam. Obviously, the induced redox reaction triggers further $^1H/^2H$ exchange in the enzyme via redox-dependent structural reorganizations of the protein. By this mechanism, H_2O molecules or protons, which are tightly bound in the oxidized state of the enzyme are loosened and made accessible to $^1H/^2H$ exchange. This interpretation would also be in line with the IR difference bands of QFR in the amide I region that have tentatively been assigned to redox-induced structural reorganizations of the enzyme (see Figure 2). With successive cycles of reduction and subsequent reoxidation, the characteristic $^1H/^2H$ exchange bands decrease in size until they totally disappear. Stable baselines are subsequently observed for the remaining experimental session. Thus, a stable equilibrium has been reached, and no further $^1H/^2H$ exchange can be induced. Yet the process of ongoing $^1H/^2H$ exchange in the spectroelectrochemical appears to be a "background reaction" with respect to the electrochemically induced redox reaction of QFR, since the observed difference spectra (baseline-corrected with respect to the $^1H/^2H$ exchange bands) do not significantly change upon progressive $^1H/^2H$ exchange. The described process of redox-induced $^1H/^2H$ exchange has previously been observed and analyzed for the cytochrome *c* oxidase from *P. denitrificans* (*50*).

Analysis of the ν(COOH) Signals in QFR WT and Variants. The focus of the present study was to analyze possible contributions of protonated glutamic and aspartic acid residues to the FTIR difference spectra of the QFR enzyme. In the context of coupled electron and proton transfer, it has been shown that the corresponding experimental results can yield extensive information about the underlying enzyme mechanism. The presented results can be compared and discussed with respect to other examples such as Glu 278 of the cytochrome *c* oxidase from *P. denitrificans* (*24*) or the corresponding Glu 286 of cytochrome bo_3 from *E. coli* (*38*) and also Glu L212 in the photosynthetic reaction center of *R. sphaeroides* (*51*, *52*). The respective band assignments in the cited studies were also accomplished with the help of site-directed mutagenesis and $^1H/^2H$ isotope exchange.

The analysis of the band pattern of the IR difference spectra in the spectral region between approximately 1745 and 1725 cm^{-1} indicates that there are contributions of several ν(COOH) modes from acidic residues (see Figures 4 and 6). This is plausible since the conservative substitution of the glutamate at position C180 with a glutamine modifies the observed signal of enzyme variant E180Q in comparison to the WT. Yet, a residual difference signal is observed at 1743 cm^{-1} for E180Q, showing that the band pattern in the WT enzyme around 1740 cm^{-1} has a more complex origin than only a single protonated side chain, namely, that of Glu C180. The occurrence of this negative signal in the reduced-minus-oxidized difference spectrum of enzyme variant E180Q indicates the protonation of least one other Glu or Asp side chain upon oxidation of the enzyme. This assignment is supported by the observed sensitivity to $^1H/^2H$ isotope exchange of this band, which has already been mentioned.

The effect of the side chain exchange is that the high-frequency carbonyl stretching vibration of the protonated carboxyl group is lost since the C═O stretching vibration of the Gln side chain absorbs at considerably lower frequencies [around ~1680 cm^{-1} (*19*)], and a possible contribution of the introduced Gln could be heavily obscured by the dominating strong difference signal in the amide I range. Thus, if residue Glu C180 was the exclusive source of this specific difference signal, which appears in the course of the induced redox reaction, then there should be no observable signal left at all in the difference spectra in this particular frequency range upon removal of the protonatable group. The existence of several protonated carboxyl groups in the QFR enzyme also explains the slight broadening of the involved overlapping difference bands in ^2H_2O (see inset of Figure 3) since the actual frequency shift upon $^1H/^2H$ isotope exchange might differ somewhat for different Asp or Glu sites within the enzyme. Furthermore, the discussed signals exhibit an increased intensity (around 1734 cm^{-1}) upon $^1H/^2H$ isotope exchange. The simplest explanation for this observation is that the overlapping bands increase the IR absorbance at the specific wavenumber. A slight increase of the involved extinction coefficients upon deuteration is also expected (*40*). Another possibility is that the pK_a value of the involved group(s) is changed in ^2H_2O (*25*).

pH Dependence of the Observed ν(COOH) Signals in QFR WT. The pH dependence of the FTIR difference signals of the QFR WT enzyme above 1715 cm^{-1} (see Figure 6) indicates that numerous groups are involved in the signal pattern, thus making it difficult to perform a detailed deconvolution of the observed signals. The fact that there are contributions of protonated glutamic and/or aspartic amino acid side chains at pH values up to pH 8.8 demonstrates the capability of the local protein environment to stabilize protonated groups at elevated pH values, which usually have p*K* values of around 4 in aqueous solution (*29*). This is in line with results from recent electrostatic calculations on the QFR from *W.* succinogenes, which allow the explicit identification of the protonation states of individual Asp and Glu side chains within the protein at neutral pH in the oxidized state of the enzyme (*46*).

Hydrogen-Bonding Strength of the Observed ν(COOH) Signals. The discussed difference signals around 1740 cm^{-1}

(see Figure 4) are indicative for protonated carboxyl groups that are moderately hydrogen-bonded and are likely to be situated inside the protein and which are thus also not directly accessible to intense hydrogen bonding with the solvent. Without any hydrogen bonds, frequencies above 1740 cm^{-1} are expected (*18*). For example, the vibration of a protonated Asp side chain without any noticeable hydrogen bond in its protein environment has been observed at 1762 cm^{-1} (*53*). A single hydrogen bond might cause a frequency decrease of 25 cm^{-1} for the involved vibration or even up to 50 cm^{-1} for strong hydrogen bonding (*40*). In general, the more surface exposed a protonated carboxyl group is, the lower is the frequency of the ν(C═O) carbonyl stretching vibration. Even signals at 1694 cm^{-1} have tentatively been assigned to ν(C═O) modes of Asp or Glu side chains (*25*, *44*).

The position of the FTIR difference signal, which has been assigned to residue Glu C180, is consistent with its location in the crystal structure of QFR as it is located near the center of transmembrane helix V and thus buried in the hydrophobic part of QFR, apparently inaccessible to bulk solvent.

Analysis of QFR WT and Variant Double Difference Spectra. Provided the conditions of the induced reactions are always identical, subtracting the difference spectra of QFR WT and the corresponding variant enzymes yields double difference spectra in which, in the ideal case, the remaining signal can solely be attributed to the differences that were induced by the single mutation. In this study, the effects of replacing Glu residues with Gln were investigated. In the context of the E-pathway hypothesis, Glu C180 is the key element. Thus, to check the protonation state of this particular residue, which is supposedly affected by the induced electrochemical redox reaction, the analysis of the resulting (double) differences focuses on the exposed IR signal of the protonated carboxyl group, since this characteristic vibration is effectively lost in the variant enzyme E180Q.

The double difference spectra WT minus E66Q and WT minus E270Q basically support the finding that WT, E66Q, and E270Q signals are very comparable. The observable nonzero signals in the double difference spectra of WT minus E66Q, which peak around 1722 cm^{-1}, may be attributed to the almost inevitable mismatch of spectra from different experiments, which cannot be overcome by simple adjustment of scaling. However, it cannot be excluded that the residual signal in the WT-minus-E66Q double difference spectrum is indeed significant and reflects protonation or environmental changes of amino acid residue Glu C66.

In the case of the WT-minus-E270Q double difference spectrum, the residual nonzero signal is negligible. Hence, it can be ruled out that Glu A270 undergoes any significant protonation changes within the framework of the performed experiment.

In contrast, the experiment with the enzyme variant E180Q shows that the protonation state of Glu C180 is directly related to the changed redox state of the heme groups (see Figures 4 and 5c). The double difference spectrum that has been calculated for WT QFR and enzyme variant E180Q data reflects the contribution of the individual amino acid residue glutamate C180 to the QFR WT signal. The signal pattern of the reduced-minus-oxidized double difference spectrum shows a maximum at 1741 cm^{-1} and a minimum at 1734 cm^{-1}, and both bands are related to residue Glu C180.

The possible origins for the observed difference signals are generally deprotonation and protonation of acidic amino acid residues or environmental changes or a superposition of both. For example, a full deprotonation of a previously fully protonated Glu or Asp side chain due to the electrochemically induced redox reaction would be reflected in the absence of the respective vibration above 1710 cm^{-1} in the FTIR spectrum of the final state, leading to a negative signal in the corresponding difference spectrum. An environmental change around protonated Glu or Asp residues would shift the respective band and thus yield a positive and negative signal of equal area (this assumes that the extinction coefficient does not change in the process) in the corresponding difference spectrum. Finally, the sign of the difference band is indicative for its affiliation to the initial (negative) or final (positive) state of the reaction.

Thus, in a basic approach, the two difference bands in the double difference spectrum WT minus E180Q can be analyzed with respect to their spectral position, sign, and area. The wavenumber is determined by the origin of the vibration, and values of 1741 and 1734 cm^{-1} are in line with vibration frequencies of protonated Asp or Glu side chains (*19*). The difference of the two numerical values (in the present case approximately 7 cm^{-1}) reflects the intensity of the induced environmental change. As mentioned above, a single H-bond can cause a decrease of 25 cm^{-1} (*40*). The area, which is enclosed by the positive and negative difference bands in the WT-minus-E180Q double difference spectrum, is not equal. Therefore, the most probable interpretation would be that amino acid residue Glu C180 undergoes a change of protonation state in the course of the induced redox reaction, which is superimposed by an environmental change of its hydrogen-bonding pattern. This proposed superimposition is plausible if the experiment (pH 7) is performed near the apparent pK_a value which, as shown experimentally, depends on the redox state of the enzyme (i.e., the applied electrode potential). On the basis of the reduced-minus-oxidized difference spectra, this means that a certain fraction of Glu C180 side chains in the population of all QFR molecules experiences complete protonation upon reduction of the hemes, whereas the remaining fraction is still protonated in the oxidized state but with a different hydrogen-bonding environment. Estimated from the amplitude of the negative peak at 1734 cm^{-1} in the reduced-minus-oxidized double difference spectrum, the fraction of Glu C180, which is protonated in the oxidized state, seems to be comparatively small with respect to the deprotonated form. The observation of a combination of a conformational change and proton uptake by Glu C180 was also obtained in recent multiconformation continuum electrostatics (MCCE) calculations (*46*).

Implications for the E-Pathway Hypothesis. In a previous study (C. R. D. Lancaster, U. S. Sauer, R. Gross, A. H. Haas, J. Graf, H. Schwalbe, W. Mäntele, J. Simon, and G. Madej, manuscript submitted for publication), we have demonstrated that the E180Q mutant is unable to support growth by fumarate respiration, and we have also shown that Glu C180 plays an essential role for the catalytic activity of the membrane-bound *W. succinogenes* QFR enzyme. The results of electrochemically induced FTIR difference spectroscopy

presented here indicate that the protonation state of Glu C180 depends on the redox state of the QFR enzyme. This supports the proposed role of Glu C180 as a key constituent of a redox-controlled transmembrane proton transfer pathway in *W. succinogenes* QFR.

In principle, it should also be possible to analyze the FTIR difference spectra obtained with respect to contributions of protonated and deprotonated heme propionates. Unfortunately, this is not easily accomplished, because protonated heme propionates absorb below 1710 cm^{-1} depending on their specific hydrogen bonding (see, for instance, ref *33*) and the (symmetric and antisymmetric) vibrations of the deprotonated species absorb in the range of the corresponding Glu and Asp vibrations. Thus, all possible heme propionate signals heavily overlap with other signals from the protein, which makes a proper assignment on the basis of the performed experiments impossible. Instead, a detailed analysis with labeled ^{13}COOH heme propionates would be necessary as has been performed in the case of the cytochrome *c* oxidase from *P. denitrificans* (*41*). If the respective signal(s) at 1692 cm^{-1} and/or 1702 cm^{-1} originate(s) from protonated heme propionates (cf. Table 1), they have to be practically inaccessible to the solvent, since they do not show the expected ^{1}H/^{2}H exchange sensitivity that would shift the corresponding vibrations to lower wavenumbers (see Figure 3).

The assignment of at least part of the electrochemically induced IR difference signal of WT QFR around 1740 cm^{-1} to the individual amino acid residue Glu C180 required site-directed mutagenesis as well as ^{1}H/^{2}H isotope exchange. Other assignments are merely tentative, and further experiments are necessary (cf. Table 1 and Supporting Information). For instance, the difference signals, which have tentatively been assigned to vibrations of protonated and deprotonated Tyr side chains, might indicate the involvement of one or more tyrosines in redox-coupled proton transfer in QFR. An assignment to specific Tyr sites in QFR on the basis of the presented data is not feasible, and further mutagenesis experiments would be required to ensure this assignment or to possibly identify an individual Tyr residue.

Even without a full assignment of all the difference signals involved, the respective IR difference spectra can be viewed as a "characteristic fingerprint" (*18*) of the investigated enzyme, with the obtained spectra being representative for QFR from *W. succinogenes* and the enzymatic redox reaction which has been induced electrochemically in the spectro-electrochemical cell.

CONCLUSIONS

In this study it was demonstrated that the diheme-containing quinol:fumarate reductase (QFR) from the anaerobic bacterium *W. succinogenes* exhibits stable and reproducible FTIR difference bands in the range from 1800 to 1000 cm^{-1} that reflect the electrochemically induced transition from the reduced to the oxidized state of the enzyme. The spectral features that can be observed in the FTIR difference spectra are fully reversible when changing from a reductive to an oxidative potential and vice versa. This indicates that the underlying redox reaction at the gold grid working electrode is also fully reversible under the applied experimental conditions. The same reversible spectral redox behavior was also ascertained in the visible difference spectra for the Soret band and α-band of the two heme groups of QFR. Of particular interest was the spectral range above 1710 cm^{-1} where ν(C═O) stretching vibrations of protonated COOH carboxyl groups absorb, because those groups can act as proton donors, respectively acceptors, and can be involved in intraprotein proton transfer reactions. It was possible to observe signals of protonated carboxyl groups originating from QFR enzyme, which either change their protonation state or experience an environmental change in the course of the induced redox reaction. This finding was supported by the fact that the relevant signals are sensitive to an isotopic ^{1}H/^{2}H exchange via the buffer solution. Furthermore, it could be shown with the help of site-directed mutagenesis that the acidic residue Glu C180 contributes to the redox-dependent signal of protonated carboxyl groups. The observed residual signal in the FTIR double difference spectrum of QFR enzyme variant E180Q and wild type can be interpreted as a protonation/deprotonation event that is superimposed by an environmental effect on the specific C═O vibration. This result provides support for the proposed role of Glu C180 within the E-pathway hypothesis of coupled transmembrane electron and proton transfer in the QFR enzyme (*15*) as an essential constituent of a transient redox-controlled transmembrane proton pathway.

ACKNOWLEDGMENT

We thank Hartmut Michel and the late Achim Kröger for long-term support of this project, Monica Sänger, Oliver Schürmann, Annette Roth for excellent technical assistance, and Michaela Ritter for assistance during the initial stages of the project. We are also grateful to Petra Hellwig for helpful comments. We thank Mauro Mileni for the determination of the quinone content of the QFR samples.

SUPPORTING INFORMATION AVAILABLE

Detailed tentative infrared band assignment including amide I and secondary structure elements, amides II and III, effects of ^{1}H/^{2}H isotope exchange, KP_i buffer, FAD/$FADH_2$, iron−sulfur clusters, hemes and heme propionates, quinones, and amino acid residues. This material is available free of charge via the Internet at http://pubs.acs.org.

REFERENCES

1. Kröger, A. (1978) Fumarate as terminal acceptor of phosphorylative electron transport, *Biochim. Biophys. Acta 505*, 129−145.
2. Lancaster, C. R. D. (2004) Structure and function of succinate: quinone oxidoreductases and the role of quinol:fumarate reductases in fumarate respiration, in *Respiration in Archaea and Bacteria, Vol. 1: Diversity of Prokaryotic Electron Transport Carriers* (Zannoni, D., Ed.) pp 57−85, Kluwer, Dordrecht, The Netherlands.
3. Mitchell, P. (1979) Keilin's respiratory chain concept and its chemiosmotic consequences, *Science 206*, 1148−1159.
4. Lemma, E., Hägerhäll, C., Geisler, V., Brandt, U., von Jagow, G., and Kröger, A. (1991) Reactivity of the *Bacillus subtilis* succinate dehydrogenase complex with quinones, *Biochim. Biophys. Acta 1059*, 281−285.
5. Lancaster, C. R. D. (2002) Succinate:quinone oxidoreductases—an overview, *Biochim. Biophys. Acta 1553*, 1−6.
6. Hägerhäll, C. (1997) Succinate:quinone oxidoreductases—Variations on a conserved theme, *Biochim. Biophys. Acta 1320*, 107−141.
7. Ohnishi, T., Moser, C. C., Page, C. C., Dutton, P. L., and Yano, T. (2000) Simple redox-linked proton-transfer design: New

insights from structures of quinol-fumarate reductase, *Structure 8*, R23−R32.
8. Lancaster, C. R. D. (2001) Succinate:quinone oxidoreductases, in *Handbook of Metalloproteins* (Messerschmidt, A., Huber, R., Poulos, T., and Wieghardt, K., Eds.) Vol. 1, pp 379−401, John Wiley & Sons, Chichester, U.K.
9. Lancaster, C. R. D. (2003) *Wolinella succinogenes* quinol:fumarate reductase and its comparison to *E. coli* succinate:quinone reductase, *FEBS Lett. 555*, 21−28.
10. Lancaster, C. R. D., Kröger, A., Auer, M., and Michel, H. (1999) Structure of fumarate reductase from *Wolinella succinogenes* at 2.2 Å resolution, *Nature 402*, 377−385.
11. Lancaster, C. R. D., Gross, R., Haas, A., Ritter, M., Mäntele, W., Simon, J., and Kröger, A. (2000) Essential role of Glu-C66 for menaquinol oxidation indicates transmembrane electrochemical potential generation by *Wolinella succinogenes* fumarate reductase, *Proc. Natl. Acad. Sci. U.S.A. 97*, 13051−13056.
12. Geisler, V., Ullmann, R., and Kröger, A. (1994) The direction of the proton exchange associated with the redox reactions of menaquinone during the electron transport in *Wolinella succinogenes*, *Biochim. Biophys. Acta 1184*, 219−226.
13. Kröger, A., Biel, S., Simon, J., Gross, R., Unden, G., and Lancaster, C. R. D. (2002) Fumarate respiration of *Wolinella succinogenes*: Enzymology, energetics and coupling mechanism, *Biochim. Biophys. Acta 1553*, 23−38.
14. Biel, S., Simon, J., Gross, R., Ruiz, T., Ruitenberg, M., and Kröger, A. (2002) Reconstitution of coupled fumarate respiration in liposomes by incorporating the electron transport enzymes isolated from *Wolinella succinogenes*, *Eur. J. Biochem. 269*, 1974−1983.
15. Lancaster, C. R. D. (2002) *Wolinella succinogenes* quinol:fumarate reductase−2.2 Å resolution crystal structure and the E-pathway hypothesis of coupled transmembrane proton and electron transfer, *Biochim. Biophys. Acta 1565*, 215−231.
16. Mäntele, W. (1993) Reaction-induced infrared difference spectroscopy for the study of protein function and reaction mechanisms, *Trends Biochem. Sci. 18*, 197−202.
17. Fabian, H., and Mäntele, W. (2002) Infrared spectroscopy of proteins, in *Handbook of Vibrational* Spectroscopy (Chalmers, J. M., and Griffiths, P. R., Eds.) Vol. 5, pp 3399−3425, John Wiley & Sons, Chichester, U.K.
18. Barth, A., and Zscherp, C. (2002) What vibrations tell about proteins, *Q. Rev. Biophys. 35*, 369−430.
19. Venyaminov, S. Y., and Kalnin, N. N. (1990) Quantitative IR spectrophotometry of peptide compounds in water (H_2O) solutions. I. Spectral parameters of amino acid residue absorption bands, *Biopolymers 30*, 1243−1257.
20. Hellwig, P., Scheide, D., Bungert, S., Mäntele, W., and Friedrich, T. (2000) FT-IR spectroscopic characterization of NADH:ubiquinone oxidoreductase (complex I) from *Escherichia coli*: Oxidation of FeS cluster N2 is coupled with the protonation of an aspartate or glutamate side chains, *Biochemistry 39*, 10884−10891.
21. Wille, G., Ritter, M., Friedemann, R., Mäntele, W., and Hübner, G. (2003) Redox-triggered FTIR difference spectra of FAD in aqueous solution and bound to flavoproteins, *Biochemistry 42*, 14814−14821.
22. Leonhard, M., and Mäntele, W. (1993) Fourier transform infrared spectroscopy and electrochemistry of the primary electron donor in *Rhodobacter sphaeroides* and *Rhodopseudomonas viridis* reaction centers: Vibrational modes of the pigments in situ and evidence for protein and water modes affected by P^+ formation, *Biochemistry 32*, 4532−4538.
23. Hellwig, P., Rost, B., Kaiser, U., Ostermeier, C., Michel, H., and Mäntele, W. (1996) Carboxyl group protonation upon reduction of the *Paracoccus denitrificans* cytochrome *c* oxidase: Direct evidence by FTIR spectroscopy, *FEBS Lett. 385*, 53−57.
24. Hellwig, P., Behr, J., Ostermeier, C., Richter, O.-M. H., Pfitzner, U., Odenwald, A., Ludwig, B., Michel, H., and Mäntele, W. (1998) Involvement of glutamic acid 278 in the redox reaction of the cytochrome *c* oxidase from *Paracoccus denitrificans* investigated by FTIR spectroscopy, *Biochemistry 37*, 7390−7399.
25. Hellwig, P., Soulimane, T., Buse, G., and Mäntele, W. (1999) Similarities and dissimilarities in the structure−function relation between the cytochrome *c* oxidase from bovine heart and from *Paracoccus denitrificans* as revealed by FT-IR difference spectroscopy, *FEBS Lett. 458*, 83−86.
26. Hellwig, P., Soulimane, T., Buse, G., and Mäntele, W. (1999) Electrochemical, FTIR, and UV/VIS spectroscopic properties of the ba_3 oxidase from *Thermus thermophilus*, *Biochemistry 38*, 9648−9658.
27. Hellwig, P., Mogi, T., Tomson, F. L., Gennis, R. B., Iwata, J., Miyoshi, H., and Mäntele, W. (1999) Vibrational modes of ubiquinone in cytochrome bo_3 from *Escherichia coli* identified by Fourier transform infrared difference spectroscopy and specific ^{13}C labeling, *Biochemistry 38*, 14683−14689.
28. Hellwig, P., Barquera, B., and Gennis, R. B. (2001) Direct evidence for the protonation of aspartate-75, proposed to be at a quinol binding site, upon reduction of cytochrome bo_3 from *Escherichia coli*, *Biochemistry 40*, 1077−1082.
29. Baymann, F., Robertson, D. E., Dutton, P. L., and Mäntele, W. (1999) Electrochemical and spectroscopic investigations of the cytochrome bc_1 complex from *Rhodobacter capsulatus*, *Biochemistry 38*, 13188−13199.
30. Ritter, M., Anderka, O., Ludwig, B., Mäntele, W., and Hellwig, P. (2003) Electrochemical and FTIR spectroscopic characterization of the cytochrome bc_1 complex from *Paracoccus denitrificans*: Evidence for protonation reactions coupled to quinone binding, *Biochemistry 42*, 12391−12399.
31. VanAken, T., Foxall-VanAken, S., Castleman, S., and Ferguson-Miller, S. (1986) Alkyl glycoside detergents: Synthesis and applications to the study of membrane proteins, *Methods Enzymol. 125*, 27−35.
32. Glasoe, P. K., and Long, F. A. (1960) Use of glass electrodes to measure acidities in deuterium oxide, *J. Phys. Chem. 64*, 188−190.
33. Moss, D. A., Nabedryk, E., Breton, J., and Mäntele, W. (1990) Redox-linked conformational changes in proteins detected by a combination of infrared spectroscopy and protein electrochemistry: Evaluation of the technique with cytochrome *c*, *Eur. J. Biochem. 187*, 565−572.
34. Mäntele, W. (1996) Infrared and Fourier transform infrared spectroscopy, in *Biophysical Techniques in Photosynthesis* (Hoff, A. J., and Amesz, J., Eds.) pp 137−160, Kluwer, Dordrecht, The Netherlands.
35. Gries, C., Hellwig, P., and Mäntele, W. (1997) Spectroelectrochemical investigations of cytochrome *c* oxidase on chemically modified semitransparent electrodes by FTIR-spectroscopy, in *Spectroscopy of Biological Molecules: Modern Trends* (Carmona, P., Navarro, R., and Hernanz, A., Eds.), Kluwer, Dordrecht, The Netherlands.
36. Allen, J. F., and Holmes, N. G. (1986) Electron transport and redox titration, in *Photosynthesis, Energy Transduction, A Practical Approach* (Hipkins, M. F., and Baker, N. R., Eds.) pp 103−141, IRL Press, Oxford and Washington, DC.
37. Rich, P. R., and Breton, J. (2001) FTIR studies of the CO and cyanide adducts of fully reduced bovine cytochrome *c* oxidase, *Biochemistry 40*, 6441−6449.
38. Lübben, M., Prutsch, A., Mamat, B., and Gerwert, K. (1999) Electron transfer induces side-chain conformational changes of glutamate-286 from cytochrome bo_3, *Biochemistry 38*, 2048−2056.
39. Foerstendorf, H., Mummert, E., Schäfer, E., Scheer, H., and Siebert, F. (1996) Fourier transform infrared spectroscopy of phytochrome: difference spectra of the intermediates of the photoreactions, *Biochemistry 35*, 10793−10799.
40. Barth, A. (2000) The infrared absorption of amino acid side chains, *Prog. Biophys. Mol. Biol. 74*, 141−173.
41. Behr, J., Hellwig, P., Mäntele, W., and Michel, H. (1998) Redox dependent changes at the heme propionates in cytochrome *c* oxidase from *Paracoccus denitrificans*: Direct evidence from FTIR difference spectroscopy in combination with heme propionate ^{13}C labeling, *Biochemistry 37*, 7400−7406.
42. Li, X.-Y., Czernuszewicz, R. S., Kincaid, J. R., Su, Y. O., and Spiro, T. G. (1990) Consistent porphyrin force field. 1. Normal-mode analysis for nickel porphine and nickel tetraphenyiporphine from resonance Raman and infrared spectra and isotope shifts, *J. Phys. Chem. 94*, 31−47.
43. Berthomieu, C., Boussac, A., Mäntele, W., Breton, J., and Nabedryk, E. (1992) Molecular changes following oxidoreduction of cytochrome *b*559 characterized by Fourier transform infrared difference spectroscopy and electron paramagnetic resonance: Photooxidation in photosystem II and electrochemistry of isolated cytochrome *b*559 and iron protoporphyrin IX-bisimidazole model compounds, *Biochemistry 31*, 11460−11471.

44. Hellwig, P., Grzybek, S., Behr, J., Ludwig, B., Michel, H., and Mäntele, W. (1999) Electrochemical and ultraviolet/visible/infrared spectroscopic analysis of heme *a* and a_3 redox reactions in the cytochrome *c* oxidase from *Paracoccus denitrificans*: Separation of heme *a* and a_3 contributions and assignment of vibrational modes, *Biochemistry 38*, 1685−1694.
45. Schlereth, D. D., and Mäntele, W. (1992) Redox-induced conformational changes in myoglobin and hemoglobin: Electrochemistry and ultraviolet−visible and Fourier transform infrared difference spectroscopy at surface-modified gold electrodes in an ultrathin-layer spectroelectrochemical cell, *Biochemistry 31*, 7494−7502.
46. Haas, A. H., and Lancaster, C. R. D. (2004) Calculated coupling of transmembrane electron and proton transfer in dihemic quinol: fumarate reductase, *Biophys. J. 87*, 4298−4315.
47. Lancaster, C. R. D. (2003) Crystallization of *Wolinella succinogenes* quinol:fumarate reductase, in *Membrane Protein Purification and Crystallization* (Hunte, C., Schägger, H., and von Jagow, G., Eds.) 2nd ed., pp 219−228, Academic Press, San Diego, CA.
48. Lübben, M., and Gerwert, K. (1996) Redox FTIR difference spectroscopy using caged electrons reveals contributions of carboxyl groups to the catalytic mechanism of haem-copper oxidases, *FEBS Lett. 397*, 303−307.
49. Lancaster, C. R. D., Gross, R., and Simon, J. (2001) A third crystal form of *Wolinella succinogenes* quinol:fumarate reductase reveals domain closure at the site of fumarate reduction, *Eur. J. Biochem. 268*, 1820−1827.
50. Hellwig, P. (1998) Elektronen- und Protonentransfer in der Cytochrom *c* Oxidase von *Paracoccus denitrificans*, Doctoral Thesis, University of Erlangen, Germany.
51. Hienerwadel, R., Grzybek, S., Fogel, C., Kreutz, W., Okamura, M. Y., Paddock, M. L., Breton, J., Nabedryk, E., and Mäntele, W. (1995) Protonation of Glu L212 following Q_B^- formation in the photosynthetic reaction center of *Rhodobacter sphaeroides*: Evidence from time-resolved infrared spectroscopy, *Biochemistry 34*, 2832−2843.
52. Nabedryk, E., Breton, J., Hienerwadel, R., Fogel, C., Mäntele, W., Paddock M. L., and Okamura, M. Y. (1995) Fourier transform infrared difference spectroscopy of secondary quinone acceptor photoreduction in proton transfer mutants of *Rhodobacter sphaeroides*, *Biochemistry 34*, 14722−14732.
53. Fahmy, K., Weidlich, O., Engelhard, M., Sigrist, H., and Siebert, F. (1993) Aspartic acid-212 of bacteriorhodopsin is ionized in the M and N photocycle intermediates—an FTIR study on specifically ^{13}C-labeled reconstituted purple membranes, *Biochemistry 32*, 5862−5869.

BI051011D